Nonlinear Thermohaline Convection

Dr. Y. RAMESHWAR

Department of Mathematics, University College of Engineering,

Osmania University, Hyderabad, India.

Our Contribution

- (1) S.G.Tagare, M.V. Ramana Murthy and Y. Rameshwar, "Nonlinear Thermohaline Convection in Rotating Fluids", IJHMT, **50**, (2007), pp.3122
- (2) Suhas Ganesh Tagare, Yadagiri Rameshwar and Shakira Sultana, "Küppers-Lortz Instability in Rotating Thermohaline Convection with Finite Prandtl Number", JPSJ, **77**, (2008), pp.104401-(1-6)
- (3) Y. Rameshwar, V. Anuradha, G. Srinivas, L.M. Pérez, D. Laroze, and H. Pleiner, "Nonlinear Convection of Binary Liquids in a Porous Medium", Chaos, **28**, (2018), pp. 075512

Motivation : H.L. Kuo, Solution of the non-linear equations of the cellular convection and heat transport, J.Fluid Mech 10 (1961) 611-630.

Abstract

- Linear and weakly nonlinear analysis of thermohaline buoyancy driven convection at the onset of stationary convection are investigated for stress free boundary conditions using perturbation analysis.
- For the stability analysis we have plotted the graphs for different values of physical parameters relevant to the ground water and oceanic water.
- To study the finite amplitude cellular convection the perturbation method is used which is proposed by Kuo[*].
- Using the solutions obtained at $O(\epsilon^8)$, the flow behaviour near the onset of stationary convection is studied.
- The effect of physical parameters is studied on heat transfer rate (Nusselt number), streamlines, isotherms and heatlines near the onset.
- It is observed the effect (stabilizing effect) of Prandtl number and Lewis number is same on the finite amplitude

Applications

- Achievements in studying natural convection are applied in [*]
- Power engineering, Metallurgy, Environmental science,
- Meteorology, Geophysics (Earths outer core, Mantle convection) and Astrophysics,
- Crystal physics, Ferrofluids, Cloud dynamics,
- Ground water, Oceanography,
- Chemical and Biological processes in fluid flows, etc.

[*] Buoyancy effects in fluids, J. S. Turner, Cambridge University Press, I973.

Physical Configuration

The fluid is contained between two extensive horizontal conducting surfaces distance d apart. The upper surface is held at the temperature T_C, and the lower surface at the higher temperature T_H.

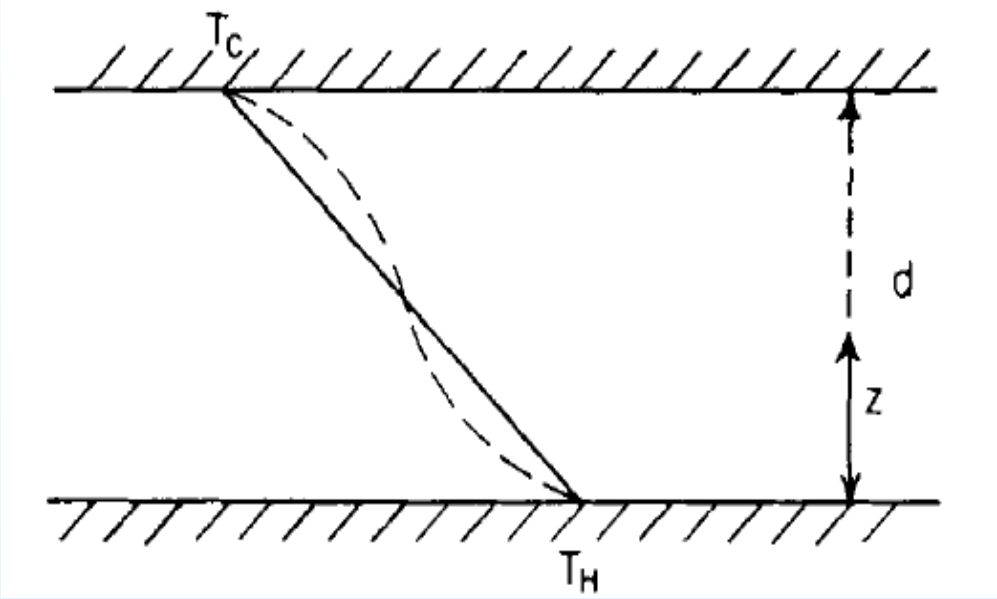

Basic Equations

The dimensional equations for thermohaline/thermosolute convection are given as [*]

$$\frac{\partial \rho}{\partial t'} + \nabla'.(\rho \vec{V}') = 0, \tag{1}$$

$$\rho \left[\frac{\partial \vec{V}'}{\partial t'} + \left(\vec{V}'.\nabla' \right) \vec{V}' \right] = -\nabla' P' + \mu \nabla'^2 \vec{V}' + \rho \vec{g}, \tag{2}$$

$$\frac{\partial T'}{\partial t'} + (\vec{V}'.\nabla')T' = \kappa_T \nabla'^2 T', \tag{3}$$

$$\frac{\partial S'}{\partial t'} + \left(\vec{V}'.\nabla' \right) S' = \kappa_S \nabla'^2 S'. \tag{4}$$

[*] Buoyancy effects in fluids, J. S. Turner, Cambridge University Press, I973.

Linear Dependence of Density

In thermohaline convection the density variations depend on both diffusive mechanisms. Thus the variation may be taken as [*], [**]:

$$\rho = \rho_0[1 - \alpha(T' - T'_b) + \beta(S' - S'_b)], \tag{5}$$

$$\rho = \rho_0[1 - \alpha(T' - T'_b) - \beta(S' - S'_b)], \tag{6}$$

with $\alpha = -\frac{1}{\rho_0}(\frac{\partial \rho}{\partial T'})$ and $\beta = \frac{1}{\rho_0}(\frac{\partial \rho}{\partial S'})$.

[*] G.Verinis, *Effect of a stabilizing gradient of solute on thermal convection,* J.Fluid Mech., **34**(1968), pp. 315.
[**] H. Rubin, *Effect of nonlinear stabilizing salinity profiles on thermal convection in a porous medium layer.* Water Resour. Res., **9**(1973), pp. 211.

Linear Dependence of Density

Here ρ_0 is the mean density of the system, T' and S' are temperature and salinity concentration of the system, α is thermal expansion coefficient and β is the coefficient of density and it increases with respect to salinity. Here T'_b is the temperature and S'_b is the salinity concentration at the bottom boundary.

Choice of Density

The choice of the density variation will depend upon the physics of the two-component system. If the heavier component of the fluid is introduced into the system, then due to diffusion of mass, there results an increase in the density of the mixture in which case the relation (5) is appropriate. If the lighter component is introduced then mass diffusion lowers the density of the mixture, hence the validity of relation (6).

The following four cases are considered (for the density variation given by eq. (5)): (a) heated from above (stabilizing) and salted from above (destabilizing); (b) heated from below (destabilizing) and salted from below (stabilizing); (c) heated from below (destabilizing) and salted from above (destabilizing); (d) heated from above (stabilizing) and salted from below (stabilizing). Here we consider the **Case (b)** is discussed in detail. It can be noted that, when salting from below the concentration decreases as the depth of the layer increases upwards.

Normal Mode Technique

(Fourier Analysis of Perturbations)

Boussinesq approximation

Case (b): Density distribution can be written in the linear approximation as

$$\rho = \rho_0[1 - \alpha(T' - T'_b) + \beta(S' - S'_b)],$$

$\alpha,\ \beta$ are defined as positive. We let the differences in temperature and salinity between the bottom and the top be ΔT and ΔS respectively and they are independent. Then if the salinity gradient is stabilizing and the temperature gradient destabilizing, we have $\Delta T > 0$, $\Delta S > 0$.

Steady State Solutions and Scaling

The conduction state is characterized by $\vec{V}' = 0$, $T'_s = T'_b - (\Delta T'/d)z'$, $S'_s = S'_b - (\Delta S'/d)z'$.

The temperature and concentration perturbations can be written as $\theta' = T' - T'_s$ and $C' = S' - S'_s$.

Scaling :

$$x = \frac{x'}{d},\ y = \frac{y'}{d},\ z = \frac{z'}{d},\ t = \frac{t'}{d^2/\kappa_T},$$

$$u = \frac{u'}{\kappa_T/d},\ v = \frac{v'}{\kappa_T/d},\ w = \frac{w'}{\kappa_T/d},\ \theta = \frac{\theta'}{\Delta T'},\ p_1 = \frac{p'_1}{\kappa_T^2 \rho_o d^{-2}}$$

and $C = C'/\Delta S'$

Dimensionless Equations

$$\nabla.\vec{V} = 0, \tag{7}$$

$$\frac{1}{Pr}\left[\frac{\partial \vec{V}}{\partial t} + \left(\vec{V}.\nabla\right)\vec{V}\right] = -\frac{\nabla p_1}{Pr} + \nabla^2\vec{V} + \left(Ra_1\theta - Ra_2 C\right)\hat{e}_z, \tag{8}$$

$$\frac{\partial \theta}{\partial t} + \left(\vec{V}.\nabla\right)\theta = w + \nabla^2\theta, \tag{9}$$

$$\frac{1}{L}\left[\frac{\partial C}{\partial t} + \left(\vec{V}.\nabla\right)C\right] = \frac{w}{L} + \nabla^2 C, \tag{10}$$

where $\hat{e}_z$ is a unit vector along z-direction.

Dimensionless Parameters

- (1) Thermal Rayleigh number : $Ra_1 = \frac{g\alpha\Delta T d^3}{\nu\kappa_T}$

Dimensionless Parameters

- (1) Thermal Rayleigh number : $Ra_1 = \frac{g\alpha\Delta T d^3}{\nu\kappa_T}$
- (2) Prandtl number : $Pr = \frac{\nu}{\kappa_T}$

Dimensionless Parameters

- (1) Thermal Rayleigh number : $Ra_1 = \frac{g\alpha\Delta T d^3}{\nu\kappa_T}$
- (2) Prandtl number : $Pr = \frac{\nu}{\kappa_T}$
- (3) Salinity Rayleigh number : $Ra_2 = \frac{g\beta\Delta S d^3}{\nu\kappa_T}$

Dimensionless Parameters

- (1) Thermal Rayleigh number : $Ra_1 = \frac{g\alpha\Delta T d^3}{\nu\kappa_T}$
- (2) Prandtl number : $Pr = \frac{\nu}{\kappa_T}$
- (3) Salinity Rayleigh number : $Ra_2 = \frac{g\beta\Delta S d^3}{\nu\kappa_T}$
- (4) Lewis number : $L = \frac{\kappa_S}{\kappa_T}$

Dimensionless Parameters

- (1) Thermal Rayleigh number : $Ra_1 = \frac{g\alpha\Delta T d^3}{\nu\kappa_T}$
- (2) Prandtl number : $Pr = \frac{\nu}{\kappa_T}$
- (3) Salinity Rayleigh number : $Ra_2 = \frac{g\beta\Delta S d^3}{\nu\kappa_T}$
- (4) Lewis number : $L = \frac{\kappa_S}{\kappa_T}$
- The four parameters Ra_1, Pr, Ra_2, and L are required for description of the motion. Here ν is the viscosity, κ_T and κ_S are the diffusivities of heat and salt. All these quantities are assumed to be constant.

Boundary Conditions

- Free-Free boundary conditions [*],[**] :

$$w = \frac{\partial^2 w}{\partial z^2} = \theta = C = 0, \qquad \text{on } \; z = 0, \; z = 1, \; \text{for all } x, y. \tag{11}$$

[*] S. Chandrasekhar, Hydrodynamic and Hydromagnetic Stability, Oxford University Press 1961.

[**] D. A. Nield, The thermohaline Rayleigh-Jeffreys problem, J. Fluid Mech. (1967), vol. 29, part 3, pp. 545-558.

Reduced PDE

The basic set of eqs.(7-10) can be reduced in to a single equation by eliminating the unknown variables $\theta,\ C$, namely we get $\mathcal{L}w = \mathcal{N}$, where

$$\mathcal{L} = \left(\frac{1}{Pr}\frac{\partial}{\partial t} - \nabla^2\right)\left(\frac{1}{L}\frac{\partial}{\partial t} - \nabla^2\right)\left(\frac{\partial}{\partial t} - \nabla^2\right)\nabla^2$$
$$-Ra_1\nabla_h^2\left(\frac{1}{L}\frac{\partial}{\partial t} - \nabla^2\right) + \frac{Ra_2}{L}\nabla_h^2\left(\frac{\partial}{\partial t} - \nabla^2\right),$$

$$\mathcal{N} = \frac{1}{Pr}\left(\frac{\partial}{\partial t} - \nabla^2\right)\left(\frac{1}{L}\frac{\partial}{\partial t} - \nabla^2\right)\hat{e}_z.\left[\nabla\times\nabla\times\left[\left(\vec{V}.\nabla\right)\vec{V}\right]\right]$$
$$+\frac{Ra_2}{L}\nabla_h^2\left(\frac{\partial}{\partial t} - \nabla^2\right)\left[\left(\vec{V}.\nabla\right)C\right] - Ra_1\nabla_h^2\left(\frac{1}{L}\frac{\partial}{\partial t} - \nabla^2\right)\left[\left(\vec{V}.\nabla\right)\theta\right].$$

Linear Stability Analysis

Near the onset of convection the growth rate of perturbations are very small, hence in the basic equations the nonlinear terms become very small compare to linear terms. Thus we neglect the nonlinear contributions from the equation $\mathcal{L}w = \mathcal{N}$. Finally we get the linear equation $\mathcal{L}w = 0$. This processes is called linearization.

We have considered motion in a plane horizontal layer and assumed that the small perturbations will be expanded in normal modes as,

$$w = W(z)e^{ikx+pt}, \quad \theta = \Theta(z)e^{ikx+pt}, \quad c = C(z)e^{ikx+pt}. \tag{13}$$

We impose the idealized boundary conditions at both interfaces of $z = 0$ and $z = 1$ (11). Hence, the boundaries dynamically stress free, and conducting to both heat and salt. Also, we have assumed periodic boundary conditions in the horizontal directions. These conditions imply that the z-dependance is contained entirely in terms of trigonometric functions. When top and bottom boundaries held at fixed concentrations (temperatures and salinities) the resulting convection takes place as a pattern of two-dimensional rolls.

- The linear equation $\mathcal{L}w = 0$ becomes after using eq.(14) as

$$\left[\left(D^2 - k^2\right)\left(D^2 - k^2 - \frac{p}{Pr}\right)\left(D^2 - k^2 - \frac{p}{L}\right)\left(D^2 - k^2 - p\right)\right] W$$
$$= \left[Ra_1 k^2 \left(D^2 - k^2 - \frac{p}{L}\right) + \frac{Ra_2 k^2}{L}\left(D^2 - k^2 - p\right)\right] W. \quad (14)$$

Rayleigh Numbers

For stationary convection, substituting $(p = 0)$ in eq. (14), we get the Rayleigh number

$$Ra_{1s} = \frac{Ra_2}{L} + \frac{(\pi^2 + k_s^2)^3}{k_s^2},$$

and minimum value of Ra_{1s} is given by
$Ra_{1s} = Ra_{1sc} = \frac{Ra_2}{L} + \frac{27\pi^4}{4}$ at $k_s = k_{sc} = \frac{\pi}{\sqrt{2}}$.

Substituting $(p = i\omega)$ in eq.(14), we get the critical Rayleigh number for oscillatory convection as

$$Ra_{1oc} = Ra_2 \frac{(L + Pr)}{1 + Pr} + \frac{(1 + L)(L + Pr)}{Pr} \frac{27\pi^4}{4} \text{ and } k_o = k_{oc} = \frac{\pi}{\sqrt{2}}. \quad (15)$$

For this model critical wavenumbers $k_{sc} = k_{oc}$, but $Ra_{1sc} \neq Ra_{1oc}$.

Plots

In Figures (1, 2) we have plotted graphs for functional relation between Ra_1 and Ra_2 to show the regions of existence of stationary and oscillatory convections for different values of $L = 0.0112, 0.01, 0.1, 0.4$ and 0.7 and $Pr = 0.01, 1, 4,$ and 7 corresponding to ground water and oceanic water. Figure 1(a) is plotted for parameter L and Pr pertaining to ground water and Figs.1(b - e) are plotted for parameter values of L and Pr corresponding to oceanic water. These figures show that as Lewis number increases for a constant value of Pr, the critical Ra_{1sc} decrease. This implies the effect of L destabilizes the convective system.

Figures 2(a-d) are plotted for increasing values of Pr for a constant value of L and it shows as Pr increases the critical value of Ra_{1oc} decrease. This implies the effect of Pr destabilizes the onset of oscillatory convection.

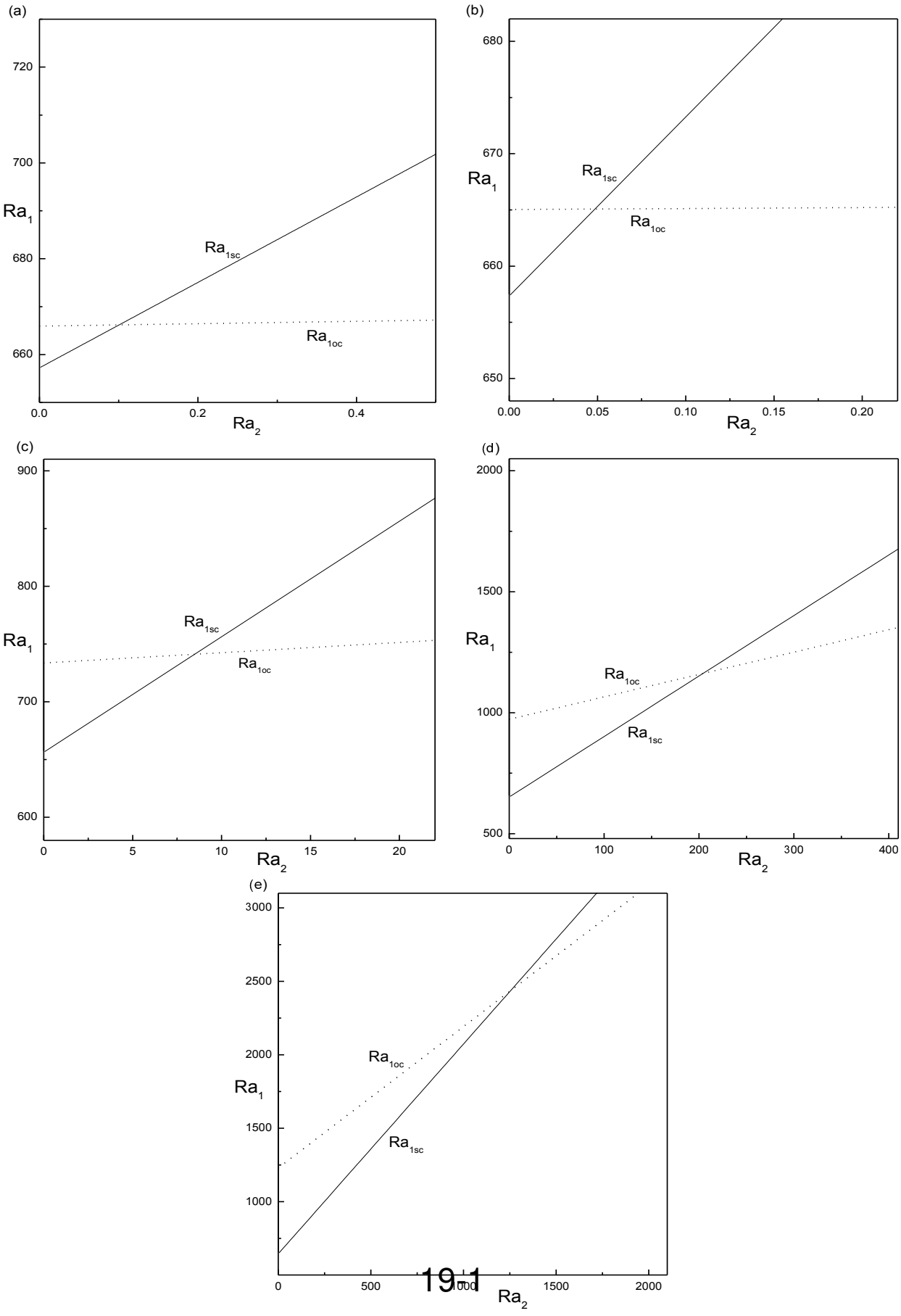
(a)
720
700
680
660
Ra1
Ra1sc
Ra1oc
0.0
0.2
0.4
Ra2
(b)
680
670
660
650
Ra1
Ra1sc
Ra1oc
0.00
0.05
0.10
0.15
0.20
Ra2
(c)
900
800
700
600
Ra1
Ra1sc
Ra1oc
0
5
10
15
20
Ra2
(d)
2000
1500
1000
500
Ra1
Ra1oc
Ra1sc
0
100
200
300
400
Ra2
(e)
3000
2500
2000
1500
1000
Ra1
Ra1oc
Ra1sc
0
500
1000
1500
2000
Ra2

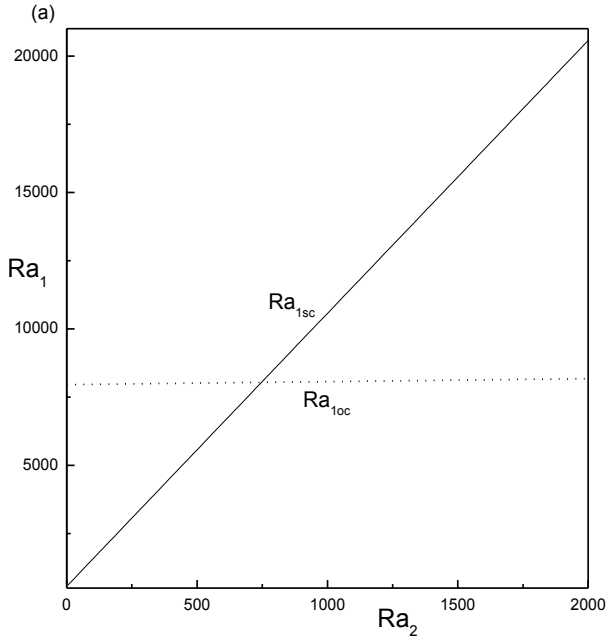
(a)
20000
15000
10000
5000
Ra1
Ra1sc
Ra1oc
0
500
1000
1500
2000
Ra2

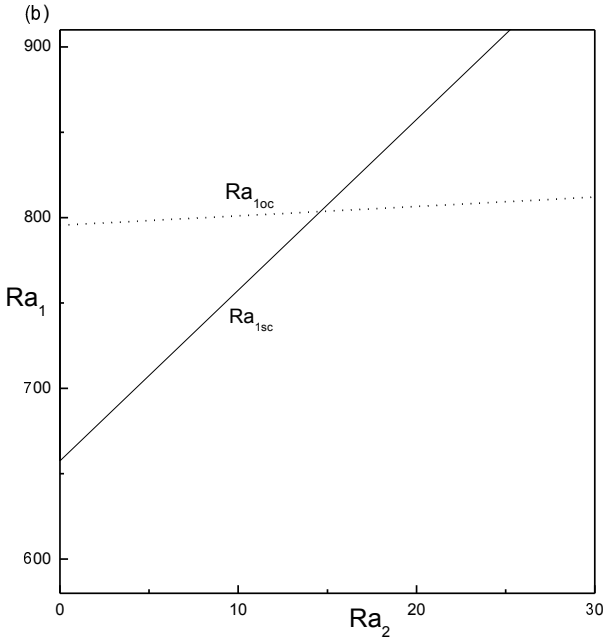
(b)
900
800
700
600
Ra1
Ra1oc
Ra1sc
0
10
20
30
Ra2

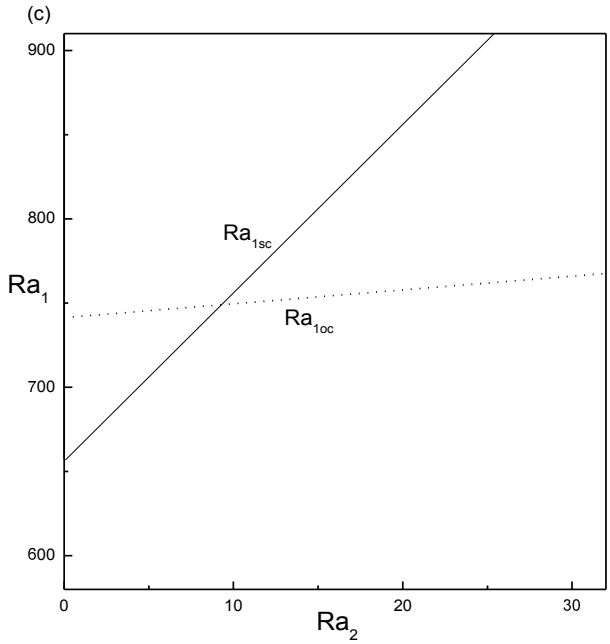
(c)
900
800
700
600
Ra1
Ra1sc
Ra1oc
0
10
20
30
Ra2

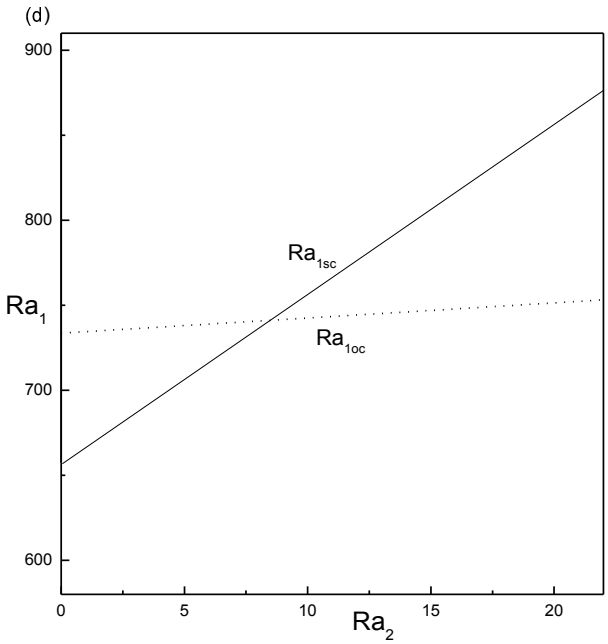
(d)
900
800
700
600
Ra1
Ra1sc
Ra1oc
0
5
10
15
20
Ra2

Finite Amplitude Cellular Convection

- When a layer of thermohaline fluid is heated uniformly from below and cooled from above, a cellular regime of steady convection is set up at values of the Rayleigh number exceeding a critical value.
- The non-linear equations describing the fields of motion, temperature and salinity concentration are expanded in a sequence of inhomogeneous linear equations dependent upon the solutions of the linear stability problem.

Finite Amplitude Cellular Convection

We have solved nonlinear equation $\mathcal{L}w = \mathcal{N}$ upto eight order using expansion $\epsilon^2 = \frac{Ra_1 - Ra_{1sc}}{Ra_1}$ proposed by Kuo[*] along

$$f = f(u, w, C, \theta) = \epsilon f_1 + \epsilon^2 f_2 + \epsilon^3 f_3 + \epsilon^4 f_4 + O(\epsilon^5), \qquad (16)$$

where f is expressed in terms eigenfunctions of the stability problem and the system is truncated to take into account only a limited number of terms.

$$Ra_1 = Ra_{1sc} + Ra_{1os}\left(\epsilon^2 + \epsilon^4 + ... + \epsilon^{2s}\right).$$

Here $Ra_{1os} = Ra_{1sc}/(1 - \epsilon^{2s})$, $s = 1, 2, 3..$ The convergence of the expansion is tested by the increasing values of s. More accurate results are obtained by retaining the higher terms in Ra_{1os}. This procedure as proposed and showed by Kuo[*] leads to a more rapid convergence.

System of Inhomogeneous Linear Equations

$$\mathcal{L}w_1 = 0, \tag{17}$$

$$\mathcal{L}w_2 = \mathcal{N}_1. \tag{18}$$

In general,

$$\mathcal{L}w_i = R_{1os}\nabla_h^2\left(\frac{1}{L}\frac{\partial}{\partial t} - \nabla^2\right)(w_{i-2}+w_{i-4}+w_{i-6}.....)+\mathcal{N}_{i-1}, \quad \text{for } i \geq 2. \tag{19}$$

Auxiliary Equations

The auxiliary equations for temperature are given by

$$\left(\frac{\partial}{\partial t} - \nabla^2\right)\theta_1 = w_1, \tag{20}$$

$$\left(\frac{\partial}{\partial t} - \nabla^2\right)\theta_2 + (\mathbf{V}_1.\nabla)\theta_1 = w_2. \tag{21}$$

In general, the auxiliary equations can be written as

$$\left(\frac{\partial}{\partial t} - \nabla^2\right)\theta_i + \sum_{l=1}^{i-1}(\mathbf{V}_l.\nabla)\theta_{i-l} = w_i, \qquad \text{for} \quad i \geq 2. \tag{22}$$

Similarly, the spectral equations for the concentration gradients are given by:

$$\left(\frac{1}{L}\frac{\partial}{\partial t} - \nabla^2\right) C_1 = \frac{1}{L} w_1, \tag{23}$$

$$\left(\frac{1}{L}\frac{\partial}{\partial t} - \nabla^2\right) C_2 + \frac{1}{L}(\mathbf{V}_1.\nabla) C_1 = \frac{1}{L} w_2. \tag{24}$$

In general, the auxiliary equations are written as

$$\left(\frac{1}{L}\frac{\partial}{\partial t} - \nabla^2\right) C_i + \sum_{l=1}^{i-1} \frac{1}{L}(\mathbf{V}_l.\nabla) C_{i-l} = \frac{1}{L} w_i, \quad \text{for } \; i \geq 2. \tag{25}$$

Solutions

The first order solutions in terms of amplitudes are given as

$$w_1 = A_1 \cos kx \sin \pi z, \tag{26}$$

$$\theta_1 = \frac{A_1}{\varpi^2} \cos kx \sin \pi z, \tag{27}$$

$$C_1 = \frac{A_1}{L\varpi^2} \cos kx \sin \pi z \tag{28}$$

$$\text{where} \quad k = k_{sc}, \quad \varpi^2 = \left(\pi^2 + k^2\right). \tag{29}$$

We express the unknown variables, w, θ and C in the following form as

$$w_i = A_i \cos kx \sin \pi z + \sum_{p,q} w_{pq}^{(i)} \cos pkx \sin q\pi z, \tag{30}$$

$$\theta_i = \frac{A_i}{\varpi^2} \cos kx \sin \pi z + \sum_{p,q} \theta_{pq}^{(i)} \cos pkx \sin q\pi z, \tag{31}$$

$$C_i = \frac{A_i}{L\varpi^2} \cos kx \sin \pi z + \sum_{p,q} C_{pq}^{(i)} \cos pkx \sin q\pi z, \tag{32}$$

where $w_{pq}^{(i)}$, $\theta_{pq}^{(i)}$ and $C_{pq}^{(i)}$ are nonlinear functions of the amplitudes A_1, A_2, A_3,.....A_{i-1}.

Expressions of Finite Amplitudes

$$A_1 = \left[\frac{8Ra_{1os}}{Ra_{1sc} - \frac{Ra_2}{L^3}}(\pi^2 + k^2)\right]^{\frac{1}{2}}, \qquad A_2 = 0. \tag{33}$$

$$A_3 = \frac{a+b}{c}, \qquad A_4 = 0. \tag{34}$$

$$a = -A_1 Ra_{1os}(1 + \pi\theta_{02}^{(2)}) - Ra_2(-\pi A_1 C_{02}^{(4)} + \pi w_{13}^{(3)} C_{02}^{(2)}),$$

$$b = Ra_{1sc}(-\pi A_1 \theta_{02}^{(4)} + \pi w_{13}^{(3)} \theta_{02}^{(2)}); \quad c = Ra_{1os} + (Ra_{1sc}\pi\theta_{02}^{(2)} - Ra_2 \pi C_{02}^{(2)}$$

$$A_{5_{at\ Ra_2=0}} = \left(\frac{Ra_{1os}}{Ra_{1sc}}\right)^{5/2}\left(\frac{0.0064}{Pr^2} + \frac{0.029}{Pr} - 0.22\right) + \left(\frac{Ra_{1os}}{Ra_{1sc}}\right)^{3/2}(1.36$$

$$+ \left(\frac{Ra_{1os}}{Ra_{1sc}}\right)^{1/2}(10.23), \qquad A_6 = 0.$$

Nusselt Number (N) Approximations

$$N = \overline{wT} - \frac{\partial \bar{T}}{\partial z}, \tag{35}$$

- $N^{(2)} = 1 + 2\epsilon^2 \left(\frac{L^3 R_{1os}}{L^3 Ra_{1sc} - Ra_2} \right),$

- $N^{(4)}{}_{(at\ Ra_2=0)} =$
  $N^{(2)}{}_{(at\ Ra_2=0)} + 2\epsilon^4 \left(\frac{Ra_{1os}}{Ra_{1sc}} \right) \left\{ 1 - 0.8335772825 \left(\frac{R_{1os}}{R_{1sc}} \right) \right\},$

- $N^{(6)}{}_{at\ Ra_2=0} =$
  $N^{(4)}{}_{at\ Ra_2=0} + 2 \left(\frac{Ra_{1os}}{R_{1sc}} \right) \left\{ 1 - 1.667 \left(\frac{Ra_{1os}}{Ra_{1sc}} \right) + S_7 \left(\frac{Ra_{1os}}{R_{1sc}} \right)^2 \right\},$

$$S_7 = \left(\frac{0.0012}{Pr^2} \right) + \left(\frac{0.0055}{Pr} \right) + 0.801 \tag{36}$$

Effect of Pr, L, Ra_2 on N

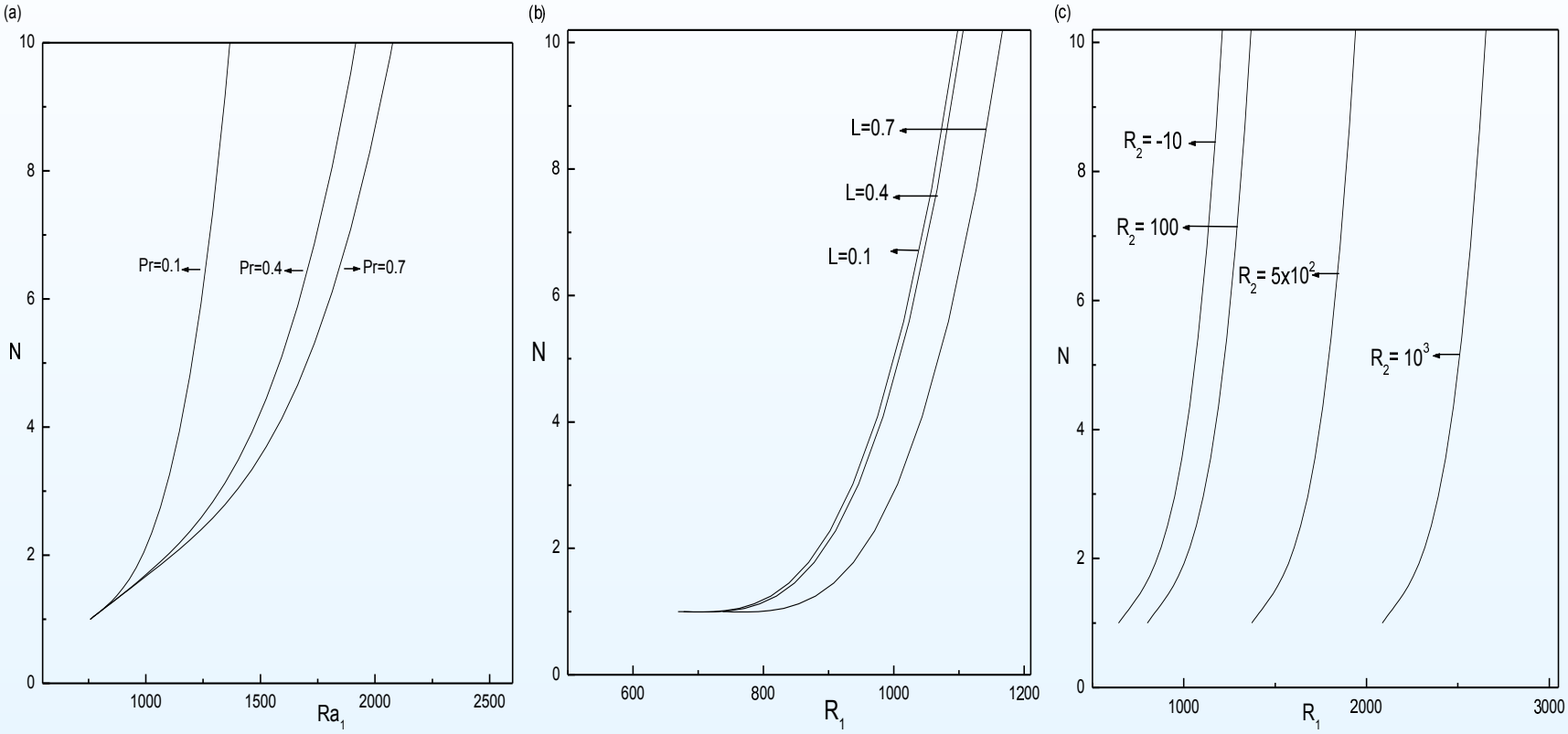

Variation of N with respect to Ra_1 (a) Plotted for different values of Pr and for fixed values of $Ra_2 = 10$ and $L = 0.1$. (b) Plotted for different values of L and for fixed values of $Pr = 7$ and $Ra_2 = 8$. (c) Plotted for different values of Ra_2 and for fixed values of $Pr = 7$ and $L = 0.7$.

Effect of Pr on N

The solutions are carried out for Prandtl numbers pertaining to Ocean and ground water, so that we can test the dependence of heat flux and other properties of the system on Prandtl number. At fixed values of the Rayleigh number, Lewis number and different values of Prandtl number we have calculated the heat flux as a function of wave-number.

- As Pr increases, the convection field gets weaken due to the higher values of kinematic viscosity. As Pr increase the heat transfer rate decreases. Hence increase in the value of Pr stabilizes the dynamical system. This result agree with those of Kuo [*] when $Ra_2 = 0$. The corresponding power law equations for $Pr = 0.1, 0.4$ and 0.7 are $N = 0.704(Ra_1/Ra_{1sc})^{4.723}$, $N = 0.702(Ra_1/Ra_{1sc})^{4.719}$ and $N = 0.702(Ra_1/Ra_{1sc})^{4.7185}$, respectively. It can be noted that for increasing Pr the power law of exponent decreases.

Effect of L on N

- It is observed that the heat transfer rate diminishes as the diffusion ratio, L increases. Hence increase in the value of L stabilizes the dynamical system. The corresponding power law equations for $L = 0.1, 0.4$ and 0.7 are $N = 0.914(Ra_1/Ra_{1sc})^{5.265}$, $N = 1.123(Ra_1/Ra_{1sc})^{4.848}$ and $N = 0.593(Ra_1/Ra_{1sc})^{3.067}$, respectively. It can be noted that for increasing L the power law of exponent decreases.

Effect of Ra_2 on N

- At a constant Ra_1, amplifying Ra_2 values always causes a decrease in the convective heat transport. Thus, it can be said that a salinity buoyancy has only damping effect on the convective heat transport. The corresponding power law equations for $Ra_2 = 100, 500$ and 1000 are $N = 0.852(Ra_1/Ra_{1sc})^{4.655}$, $N = 1.139(Ra_1/Ra_{1sc})^{5.980}$ and $N = 1.391(Ra_1/Ra_{1sc})^{7.495}$, respectively.

Streamlines and Isotherms

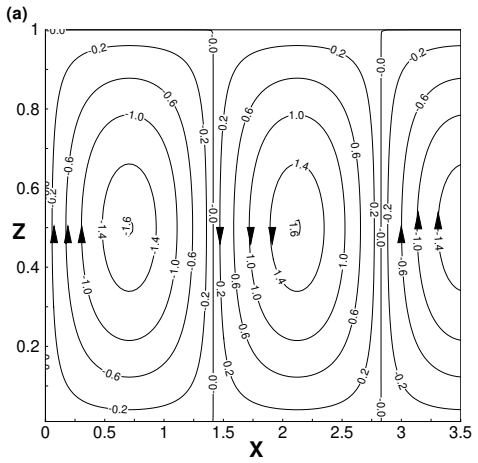

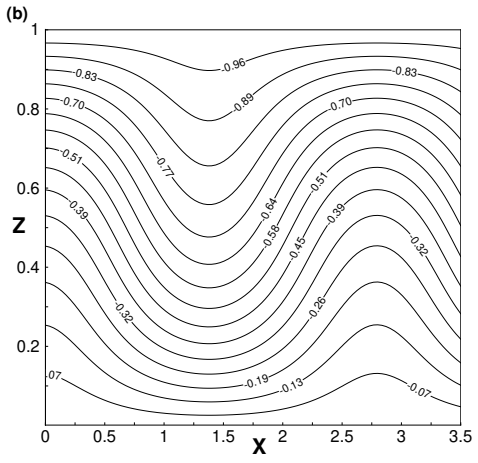

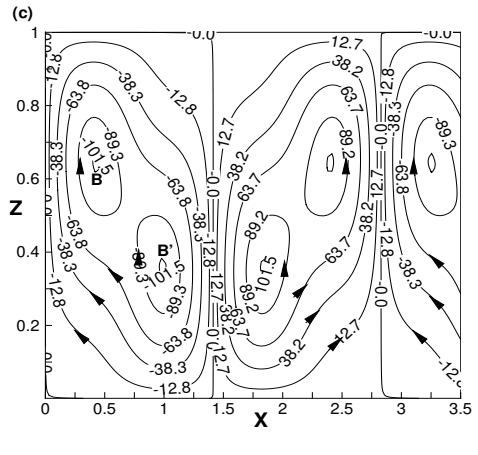

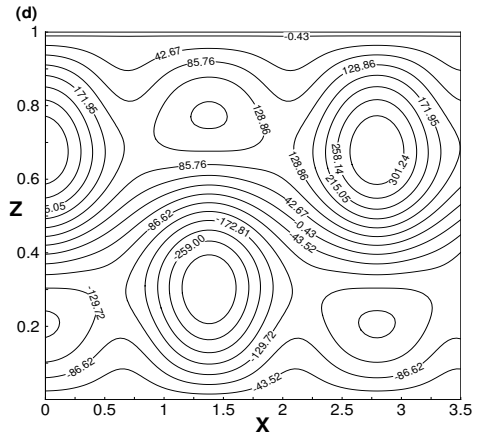

Effect of Ra_1 for $Pr = 7$, $L = 0.7$ and $Ra_2 = 10$. Streamlines (a, c) and isotherms (b, d). (a),(b) are plotted for $Ra_1 = 1.1Ra_{1sc}$, (c),(d) are plotted for $Ra_1 = 25Ra_{1sc}$.

Streamlines and Isotherms

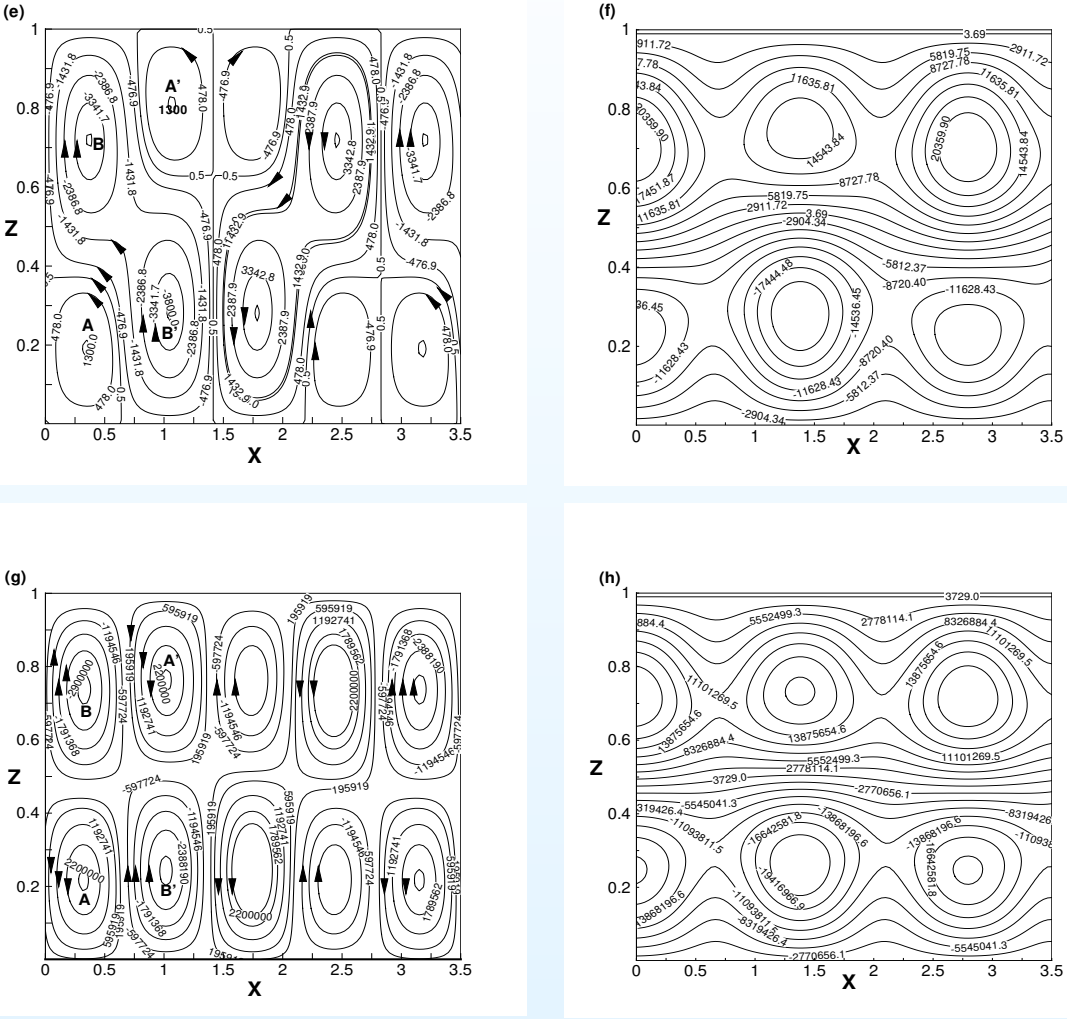

Effect of Ra_1 for $Pr = 7$, $L = 0.7$ and $Ra_2 = 10$. Streamlines (e, g) and isotherms (f, h). (e),(f) are plotted for $Ra_1 = 100Ra_{1sc}$ and (g),(h) are plotted for $Ra_1 = 1000Ra_{1sc}$.

Circulation Strength of a Cell

$0 < X < 1.4, 0 < Z < 1$	Absolute Maximum	Absolute minimum
$Ra_1 = 1.1Ra_{1sc}$	1.593	0.0002699
$Ra_1 = 25Ra_{1sc}$	101.93	0.0422
$Ra_1 = 100Ra_{1sc}$	1300	-3819.14
$Ra_1 = 1000Ra_{1sc}$	2.98321×10^6	-2.98501×10^6

Fluid flow rate increase as the thermal Rayleigh number, Ra_1 increases.

Streamlines and Isotherms

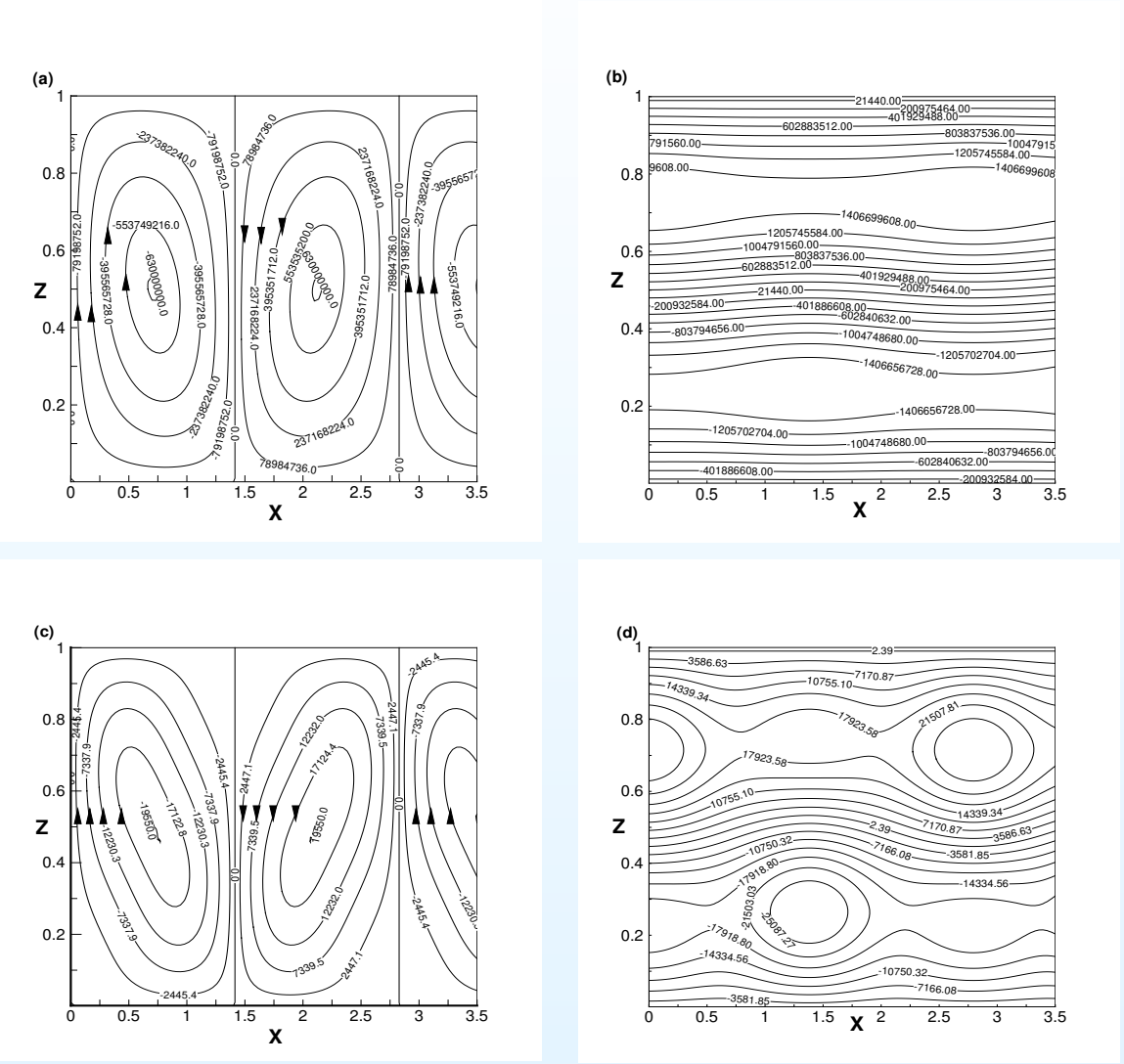

Effect of Ra_2 for $Pr = 7$, $L = 0.7$ and $Ra_1 = 50Ra_{1sc}$.
Streamlines (a, c) and isotherms (b, d). (a), (b) are plotted for $Ra_2 = 400$, (c),(d) are plotted for $Ra_2 = 100$.

Streamlines and Isotherms

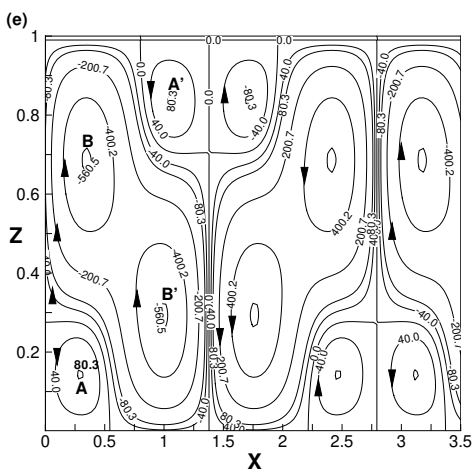

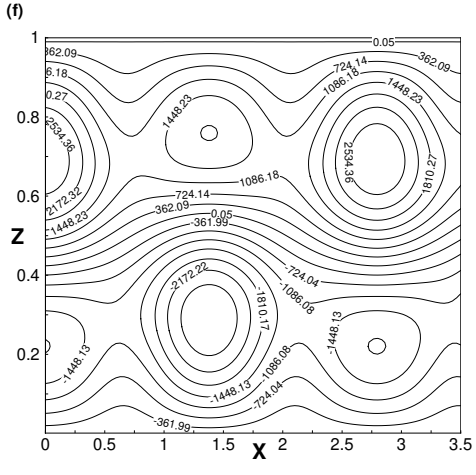

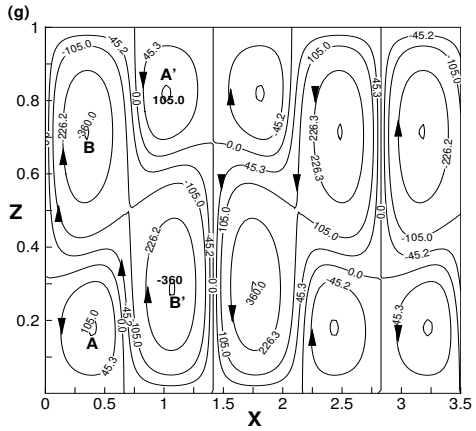

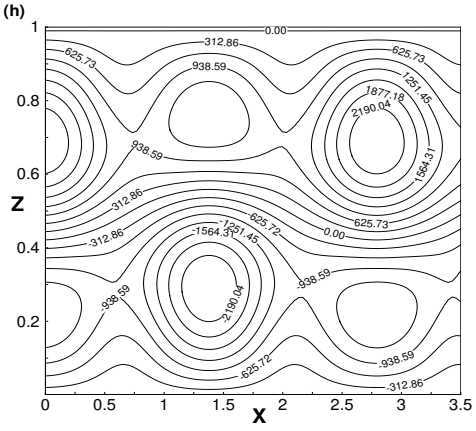

Effect of Ra_2 for $Pr = 7$, $L = 0.7$ and $Ra_1 = 50Ra_{1sc}$. Streamlines e, g) and isotherms (f, h). (e),(f) are plotted for $Ra_2 = 10$ and (g),(h) are plotted for $Ra_2 = 5$.

Circulation Strength of a Cell

$0 < X < 1.4,\ 0 < Z < 1$	Absolute Maximum	Absolute minimum
$Ra_2 = 400$	-107008	-6.32841×10^8
$Ra_2 = 100$	-0.822266	-19569
$Ra_2 = 10$	80.3	-560
$Ra_2 = 5$	105	-360

Fluid flow rate decrease as the salinity Rayleigh number, Ra_2, increases.

Heatfunction

The heatlines are similar to the streamlines and they help us to visualize the net energy flow in a heat transfer enhanced convection or conduction situation. Heatline technique is one of the significant methods to visualize the heat transport in a convective model and it acts as an effective tool for the visualization of convective heat transfer in the flow regime. It is worth mentioning that in 1983 Kimura and Bejan have developed the heatline analysis [*].

For the considered non-dimensional convection problem Heatfunction (H^*) can be obtained from the following equations:

$$\frac{\partial H^*}{\partial x} = wT - \frac{\partial T}{\partial z}, \quad -\frac{\partial H^*}{\partial z} = uT - \frac{\partial T}{\partial x},$$

[*] S. Kimura, A. Bejan, The heatline visualization of convective heat transfer, J. Heat Transfer **105** (1983), pp. 916-919.

Boundary Conditions

The following boundary conditions for H^* are obtained from the integration of the expressions for the H^* derivatives:

At $z = 0, 0 \leq x \leq \pi/k : H^*(x,0) = H^*(0,0) + \int_0^x \left(wT - \frac{\partial T}{\partial z} \right) dx,$

At $z = 1, 0 \leq x \leq \pi/k : H^*(x,1) = H^*(0,1) + \int_0^x \left(wT - \frac{\partial T}{\partial z} \right) dx,$

At $x = 0, 0 \leq z \leq 1 : H^*(0,z) = H^*(0,0) - \int_0^z \left(uT - \frac{\partial T}{\partial z} \right) dz,$

At $x = \pi/k, 0 \leq z \leq 1 : H^*(\pi/k,z) = H^*(\pi/k,0) - \int_0^z \left(uT - \frac{\partial T}{\partial x} \right) dz.$

Effect of Ra_1 on Heatlines

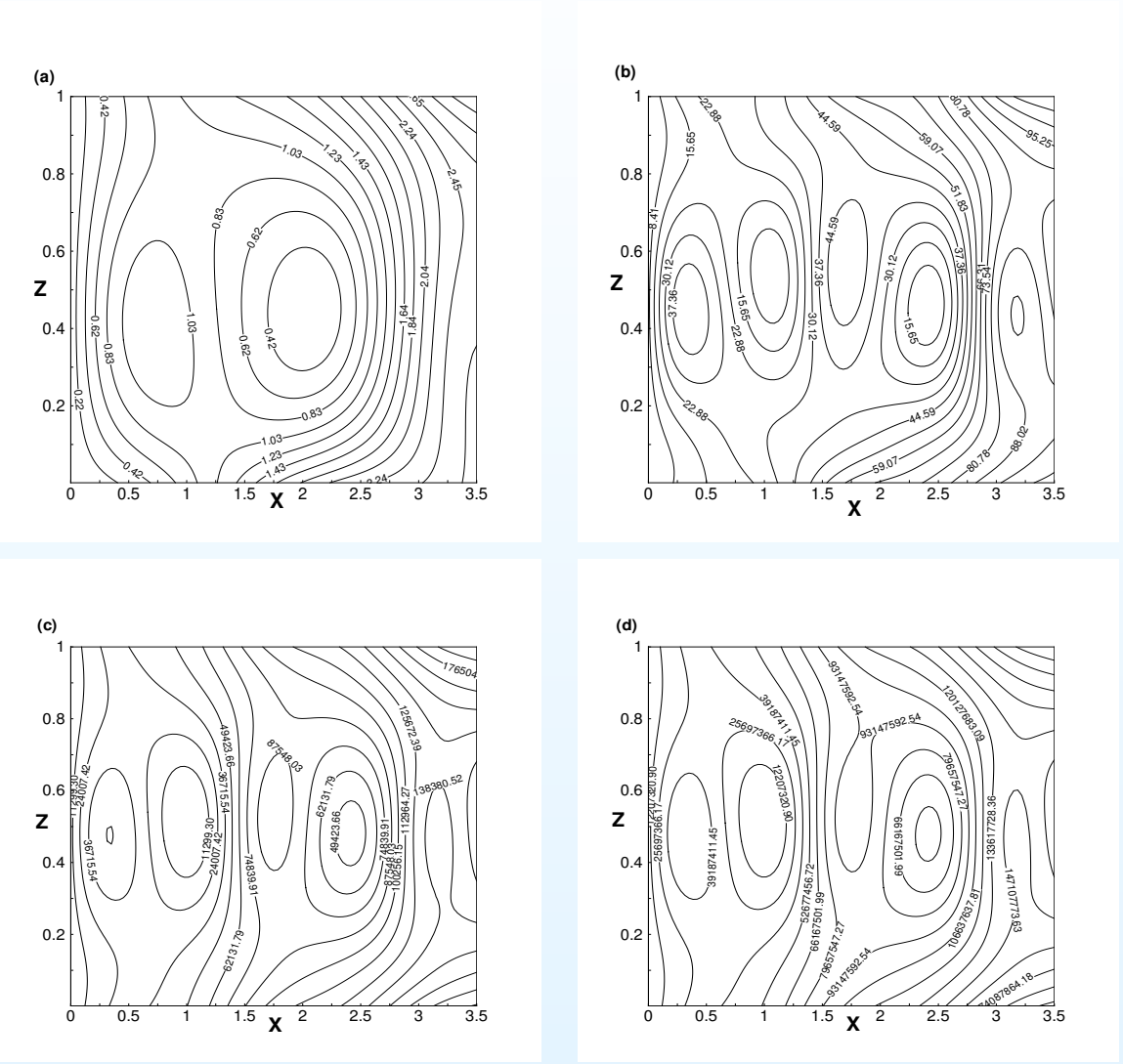

Heatlines drawn for $Pr = 7$, $L = 0.7$ and $Ra_2 = 10$,
(a)$Ra_1 = 1.1Ra_{1sc}$ (b)$Ra_1 = 10Ra_{1sc}$ (c)$Ra_1 = 100Ra_{1sc}$
(d)$Ra_1 = 1000Ra_{1sc}$.

Net Energy Flow

	Absolute Minimum	Absolute Maximum
$Ra_1 = 1.1Ra_{1sc}$	0.22	2.65
$Ra_1 = 10Ra_{1sc}$	8.41	95.25
$Ra_1 = 100Ra_{1sc}$	11299.3	176504
$Ra_1 = 1000Ra_{1sc}$	22073209	147107773.6

Net energy flow rate increase as Rayleigh number, Ra_1, increases.

Effect of Pr on Heatlines

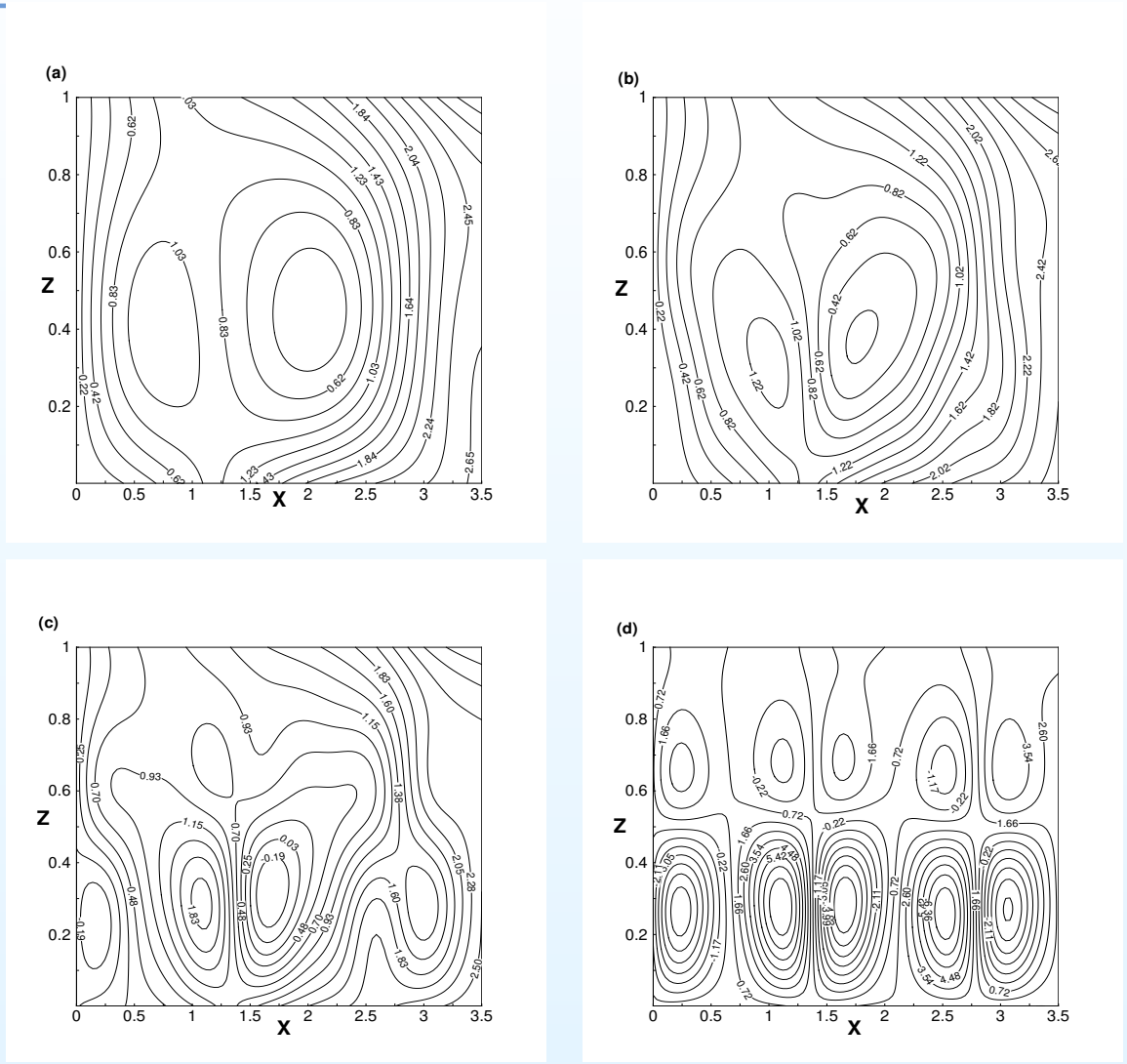

Heatlines drawn for $Ra_1 = 1.1Ra_{1sc}$, $L = 0.7$ and $Ra_2 = 10$,
(a)$Pr = 0.1$ (b)$Pr = 0.015$ (c)$Pr = 0.01$ (d)$Pr = 0.005$.

Near the onset

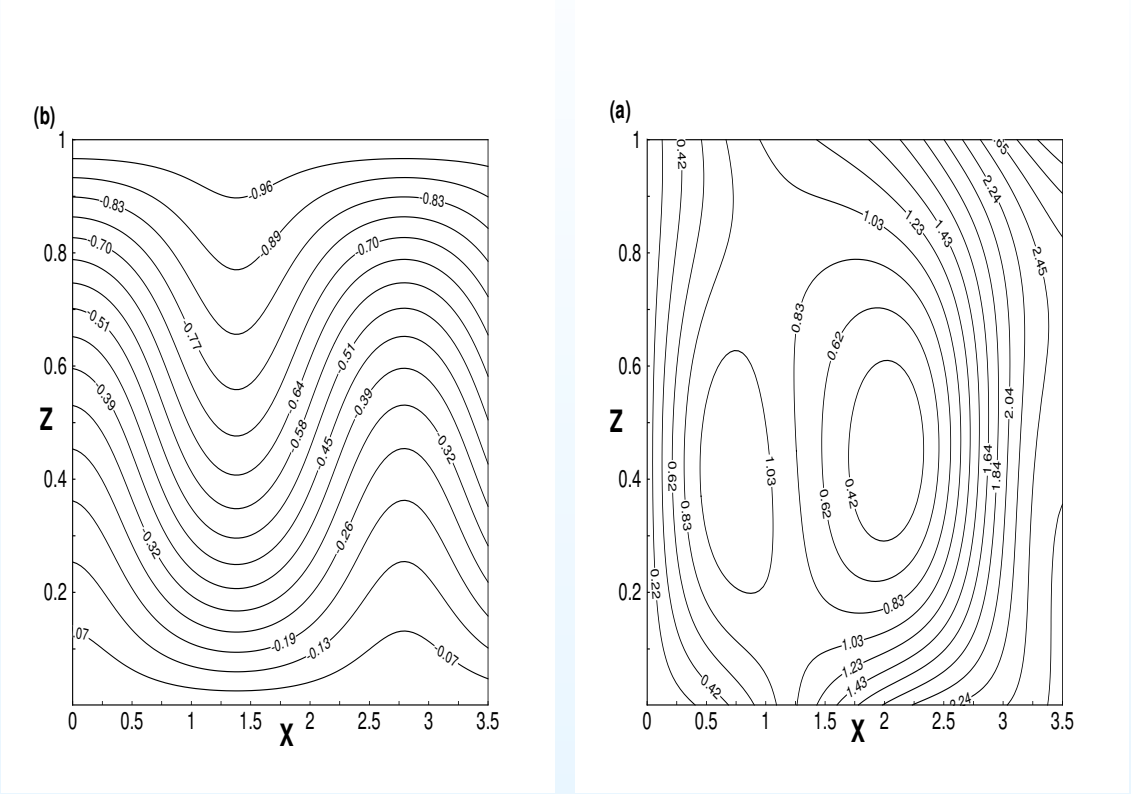

Streamlines (left), isotherms (middle) and heatline (right) for $Pr = 7$, $L = 0.7$ and $R_2 = 10$, $R_1 = 1.1R_{1c}$.

Similarity

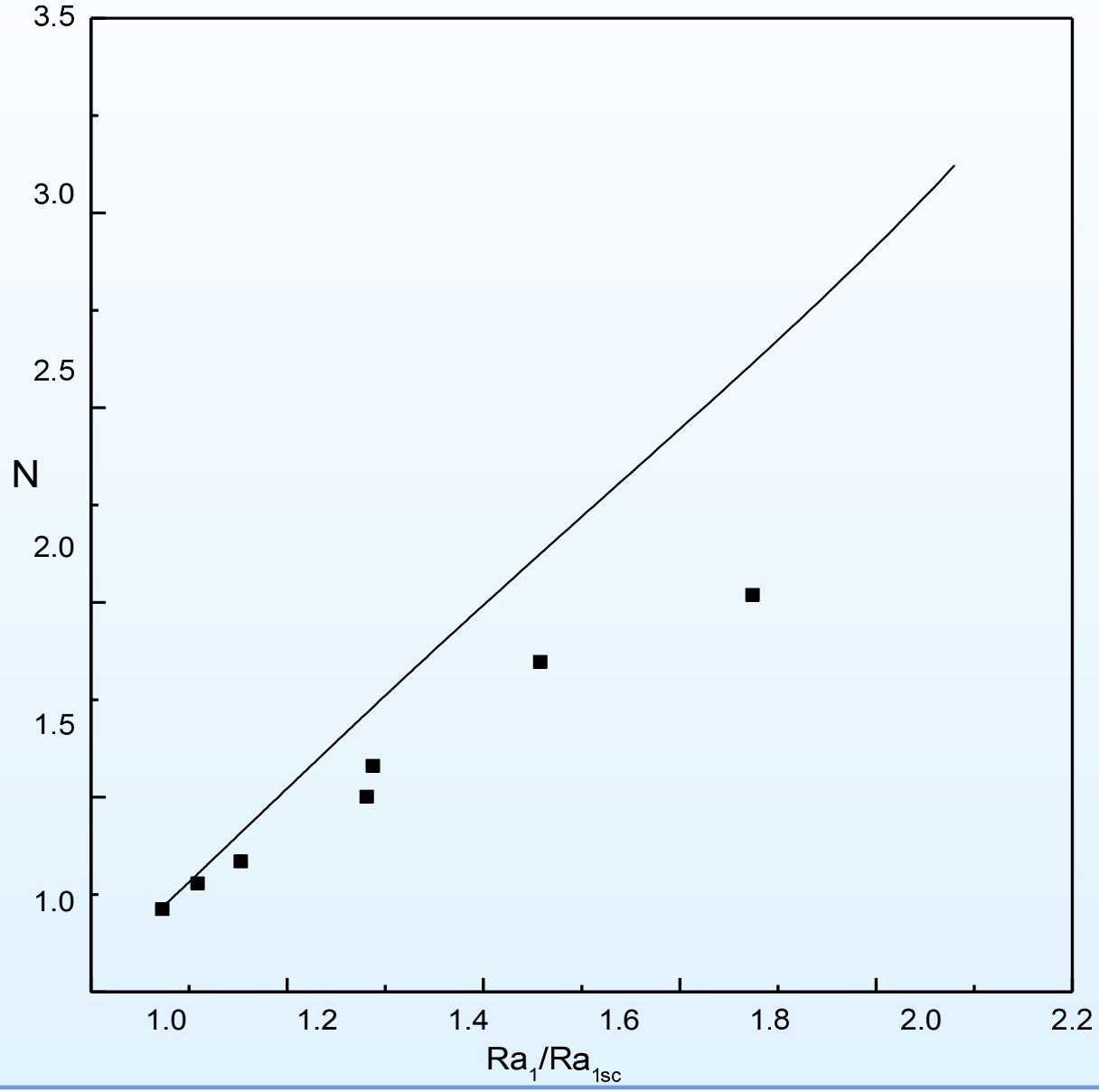

Conclusions

- The solution of this physical model is evaluated and analysed by using the normal mode technique.
- From the linear stability analysis we observed the occurrence of both stationary convection and oscillatory convection. These convective instabilities strongly depends on Pr.
- For $L < 1$ and increase from 0.1 to 0.7, the critical Ra_{1sc} decreases. This implies the effect of L destabilizes the convective system.
- As Pr increases, the critical value of Ra_{1oc} decrease. This implies the effect of Pr destabilizes the onset of oscillatory convection.
- The amplitudes are derived until the eighth order using the iterative method proposed by Kuo [*].

Conclusions

- It is observed that heat transfer rate diminishes as the diffusion ratio L increases.
- It is observed that heat transfer rate decrease as Pr increases.
- It is observed that the amplifying $Ra_2 > 0$ values causes for the decrease in the convective heat transport across the layer.
- Near the onset, the convective stationary rolls are observed and dependent upon the temperature difference and concentration difference across the fluid layer. These stationary rolls become either periodic or chaotic under the influence of parameters.
- It is observed that the numerical values of Heatfunction are closely related to the average Nusselt number. The intensity of heat flow circulation is decreased due to the increase in Pr, L and Ra_2.

References

- M.E. Stern, The salt fountain and thermohaline convection. Tellus, 1960; 12: 172-5 (pp 253,258).
- G. Veronis, On finite amplitude instability in thermohaline convection, J.Marin.Res., 1965; 23: 1-17 (pp 253,259).
- H. Stommel, A. B. Arons, D. Blanchard, An ocean curiosity: the perpetual salt fountain, Deep-Sea Res., 1956; 3: 152–153.
- D.A. Nield, The thermohaline Rayleigh-Jeffreys problem, J. Fluid Mech., 1967; 29:(03), 545-558.
- J.S. Turner, Multicomponent convection, An. Rev. Fluid Mech., 1985; 17: 11-44.
- Baines, P.G. Gill, A.E., On thermohaline convection with linear gradients, J.Fluid Mech 37: 1969; 289-306.
- H. E. Huppert, D. R. Moore, Nonlinear double-diffusive convection, J. Fluid Mech., 1976; 78:(4) 821-854.

References

- H.L. Kuo, Solution of the non-linear equations of the cellular convection and heat transport, J.Fluid Mech 10 (1961) 611-630.
- S. Kimura, A. Bejan, The heatline visualization of convective heat transfer, J. Heat Transfer 105 (1983) 916-919.
- S. Chandrasekhar, Hydrodynamic and Hydromagnetic Stability, Oxford University Press 1961.
- Al.M. Morega, A. Bejan, Heatline visualization of forced convection laminar boundary layers, Int. J. Heat Mass Transfer 36 (1993) 3957-3966.
- V.A.F. Costa, Bejan's heatlines and masslines for convection visualization and analysis, Appl. Mech. Rev. 59 (2006) 126-145.

References

- H.P. Rani, G. Janardhan Reddy, C.N. Kim, Y. Rameshwar, Transient couple stress fluid past a vertical cylinder with Bejan's heat and mass flow visualization for steady-state, J. Heat Transfer 137(3) (2015) 032501.
- T. Basak, S. Roy, Role of Bejan's heatlines in heat flow visualization and optimal thermal mixing for differentially heated square enclosures, Int. J. Heat Mass Transfer 51 (2008) 3486-3503.
- Y.Rameshwar, M.A.Rawoof Sayeed, H.P.Rani, D.Laroze, Finite amplitude cellular convection under the influence of a vertical magnetic field, Int.J. Heat and Mass Transfer 114 (2017) 559-577.

END